A biophysical and structural analysis of DNA binding by oligomeric hSSB1 (NABP2/OBFC2B)

Serene El-Kamand[1], Slobodan Jergic[2], Teegan Lawson[1], Ruvini Kariawasam[1], Derek J. Richard[3], Liza Cubeddu[1,4*] and Roland Gamsjaeger[1,4*]

[1]School of Science, Western Sydney University, Penrith, NSW 2751, Australia
[2]Molecular Horizons and School of Chemistry and Molecular Bioscience, University of Wollongong, and Illawarra Health and Medical Research Institute, Wollongong, NSW 2522, Australia
[3]School of Biomedical Research, Institute of Health and Biomedical Innovation at the Translational Research Institute, Queensland University of Technology, Woolloongabba, QLD 4102, Australia
[4]School of Life and Environmental Sciences, University of Sydney, Sydney, NSW 2006, Australia

*Corresponding authors: Liza Cubeddu and Roland Gamsjaeger
E-mails: L.Cubeddu@westernsydney.edu.au and R.gamsjaeger@westernsydney.edu.au

Running title: DNA binding by oligomeric hSSB1

Keywords: DNA repair, nuclear magnetic resonance (NMR), protein structure, protein-DNA interaction, oligomerization

Abstract
The oxidative modification of DNA can result in the loss of genome integrity and must be repaired to maintain overall genomic stability. We have recently demonstrated that human single stranded DNA binding protein 1 (hSSB1/NABP2/OBFC2B) plays a crucial role in the removal of 8-oxo-7,8-dihydro-guanine (8-oxoG), the most common form of oxidative DNA damage. The ability of hSSB1 to form disulphide-bonded tetramers and higher oligomers in an oxidative environment is critical for this process. In this study, we have used nuclear magnetic resonance (NMR) spectroscopy and surface plasmon resonance (SPR) experiments to determine the molecular details of ssDNA binding by oligomeric hSSB1. We reveal that hSSB1 oligomers can open up damaged dsDNA and interact with individual single strands; however, our data also show that oxidised bases are recognised in the same manner as undamaged DNA bases. NMR experiments provide evidence that oligomeric hSSB1 is able to bind longer ssDNA in both binding polarities using a distinct set of residues different to those of the related SSB from *Escherichia coli*. We further demonstrate that oligomeric hSSB1 recognises ssDNA with a significantly higher affinity than its monomeric form and propose structural models for oligomeric hSSB1-ssDNA interaction.

Introduction
Cells are subjected to constant oxidative stress that can damage the integrity of the genome and lead to diseases including cancer (1,2). To maintain genomic stability, oxidative DNA damage must be repaired before replication and cell division can occur.
The oxidation of guanine, the most commonly modified DNA base, results in the formation of the highly mutagenic 8-oxo-7,8-dihydro-guanine (8-oxoG) (3-6). Additional to the canonical Watson-Crick base pairing with cytosine, 8-oxoG has the ability to form stable Hoogsteen pairs with adenine, meaning that a G:C to A:T transversion may occur during replication as a result of this base modification (7).
Base excision repair (BER) is the main mechanism responsible for preventing the build-up of 8-oxoG in the human genome (8). In the BER process, human oxoguanine glycosylase 1 (hOGG1) first acts as a DNA glycosylase, cleaving the *N*-glycosidic bond, then functions as an apurinic/apyrimidinic (AP) nuclease, removing the 3' phosphate of the resulting abasic site (9). DNA polymerase beta (POLβ) replaces the removed 8-oxoG nucleotide with a guanine residue that is ligated in place by the action of DNA ligase III (10).
Single stranded DNA binding proteins (SSBs) bind to and protect ssDNA in DNA processing events including DNA repair (11,12). Human SSB1 has previously been found to function in double strand break (DSB) repair, forming part of the sensor of single-stranded DNA complex 1 (SOSS1 complex) (13-15). More recent studies have found that hSSB1 is also involved in the removal of 8-oxoG from the genome, playing a central role in the recruitment of hOGG1 to damaged chromatin after oxidative damage (16).
hSSB1 monomers contain a single, highly conserved OB fold at the N-terminus followed by a flexible spacer region and a conserved C-terminal tail that is involved in protein-protein interactions (17,18). There are three cysteine residues present in the OB fold of hSSB1, two of which are solvent exposed (C81 and C99) (19). These cysteine residues, along with a set of charged and polar residues within the OB domain of hSSB1, facilitate the oligomerisation of hSSB1 under oxidative conditions, where hSSB1 forms homo-tetramers and larger oligomers (20,21). Our model of hSSB1 oligomerisation has also revealed that monomer-monomer and dimer-dimer interactions stabilising the hSSB1 tetramer occur at distinct surfaces of the OB domain that do not overlap with the ssDNA binding surface, indicating that ssDNA recognition by stable hSSB1 tetramers may be possible.
However, despite its significant functional importance, the exact molecular details of DNA binding by oligomeric hSSB1 remains unknown. In this study, we utilise solution-state nuclear magnetic resonance (NMR) spectroscopy and surface plasmon resonance (SPR) to elucidate the structural and biophysical details of the oligomeric hSSB1-DNA interaction.

Results
Oligomeric hSSB1 is able to open up dsDNA containing 8-oxoG damage

We have previously observed that oxidised hSSB1 (referred to as 'oligomeric hSSB1' in this study based on our previous work (21)) displays an increased binding affinity when recognising dsDNA containing a single 8-oxoG (19). To test this further, 1D and 2D spectra of (assigned) 8-oxoG containing dsDNA (to mimic oxidative DNA damage) were analysed in the absence and presence of oligomeric $hSSB1_{1-123}$ (Figure 1).
To first examine if the two dsDNA strands separate before protein binding occurs, a solution of ^{15}N-$hSSB1_{1-123}$ bound to 8-oxoG dsDNA was subjected to HSQC NMR experiments. These spectra were compared to experiments recorded with single stranded oligo$(dT)_{12}$ ssDNA (Figure 1A). Not surprisingly, the position of hSSB1 residues is mostly conserved, revealing that the protein recognises exposed ssDNA, which demonstrates that oligomeric $hSSB1_{1-123}$ does not directly bind dsDNA but rather opens up the DNA double helix. In addition, these data indicate that the presence of the 8-oxoG base does not change the underlying molecular mechanism (i.e., base stacking) of protein binding.
Next, to determine which part of the dsDNA is opened up by protein binding, we recorded 1D and 2D NOESY experiments of the dsDNA in the absence and presence of oligomeric $hSSB1_{1-123}$. Figure 1B shows a section of a 1D spectrum (12-14.5 ppm) that contains assigned imino protons participating in regular Watson-Crick bonds indicative of intact dsDNA. Apart from peak broadening consistent with protein binding, significant chemical shift changes were seen in the peaks correlating to the DNA bases G4, T36 and G37 (Figure 1B), which are all located on the left-hand side (referred to as LHS in Figure 1B) of the 8-oxoG base in the dsDNA sequence. These data strongly indicate that hSSB1 opens up a portion of the duplex by binding to the single strands on the right-hand side (RHS) of the 8-oxoG base (Figure 1C), eliminating signals from the bases on the RHS of the sequence and causing a change in environment for the bases on the LHS, which have remained Watson-Crick bonded. However, it is not clear how hSSB1 oligomers structurally recognise the exposed ssDNA (as indicated by the questions marks in Figure 1C).

The presence of an oxidised guanine does not change the oligomeric hSSB1 binding mechanism
To further confirm that the presence of 8-oxoG does not change the structural details of ssDNA recognition, HSQC experiments of oligomeric ^{15}N-$hSSB1_{1-123}$ were recorded in the presence ((oligo$(dT)_5$oxoG) with the sequence of [5′-TToxoGTTT-3′]) and absence (oligo$(dT)_6$) of 8-oxoG, respectively (Figure 2A, B). Both the direction and the magnitude of the shift in the backbone moieties are conserved (Figure 2A-D), suggesting that the presence of the oxidised guanine base does not affect the underlying molecular mechanism. This result is not unexpected, as DNA recognition by hSSB1 is modulated by base-stacking with ssDNA bases (20) and the oxidation of the guanine base does not alter its ability to stack with any of the key aromatic residues in hSSB1.

Oligomeric hSSB1 can bind ssDNA in both binding polarities
In previous work, we have shown that the OB domain of the SSB from *Sulfolobus solfataricus* SSB (SsoSSB) interacts with ssDNA with a specific binding polarity (22). Both hSSB1 and SsoSSB use a combination of base-stacking between aromatic residues and ssDNA bases, as well as some hydrogen bonding to bind ssDNA. While base-stacking does not confer any directionality on ssDNA binding, most SSBs have a preferred binding orientation (23). Although both our NMR structure (20) and the published crystal structure (18) indicate a preferred binding polarity, no other experimental data have been obtained to exclude the possibility that a second conformer, which binds ssDNA in the reverse direction to that observed in the published structures, exists.
To address this, we carried out a semi-quantitative analysis using paramagnetic resonance enhancement (PRE) labelled ssDNA oligomers [5′-G'(PRE)'GTTTTTT-3′] (see experimental section for more details), in analogy to our published approach with SsoSSB (22) (Figure 3). Figure 3A depicts an overlay of a HSQC spectrum of oligomeric ^{15}N-$hSSB1_{1-123}$ in the presence of unlabelled ssDNA (diamagnetic conditions, labelled 'control' in Figure) onto a HSQC spectrum of ^{15}N-$hSSB1_{1-123}$ in the presence of PRE-labelled ssDNA (paramagnetic conditions, labelled 'PRE' in Figure). Calculation of the ratio between peak intensities of 'PRE' and 'control' conditions (Figure 3B) revealed residues that either exhibit no signal in the presence of PRE-ssDNA or undergo substantial decreases in their peak intensities (indicated as red bars in the Figure) and are thus located in close proximity to the PRE-label. These residues were mapped onto our published hSSB1 tetramer model (coloured in red in Figure 3C, D). We have previously also calculated a structural model of

monomeric hSSB1 bound to ssDNA (oligo$(dT)_6$) (20). To visualise where in the tetrameric structure ssDNA binding most likely occurs, our published model (20) was overlaid onto all four monomers within the tetramer model; the ssDNA is shown in blue in Figure 3C.
Notably, all residues that are within a small distance from the paramagnetic nitroxide spin-label are found in regions where the protein is closest to either the 3′ or the 5′ end of the ssDNA. Given the PRE-label is covalently bound to the 5′ end of the ssDNA these data strongly indicate that, as opposed to SsoSSB, oligomeric hSSB1 is able to bind to ssDNA utilising both binding polarities.

hSSB1 binds to longer strands of DNA as an oligomer
We have shown that oligomeric hSSB1 is able to open up dsDNA and interact with single strands of DNA (Figure 1). However, it is not clear from those data how the formation of hSSB1 oligomers affects ssDNA recognition. For example, the question remains whether hSSB1 tetramers can directly bind to ssDNA or if binding takes place through assembly by addition of successive monomers on to ssDNA of increasing length.
To address this, we carried out 1D NMR experiments of oligo$(dT)_{12}$ ssDNA (instead of short oligo$(dT)_6$) in complex with oligomeric hSSB1. Figure 4 shows sections of 1D spectra that contain peaks for the H1 sugar protons of the ssDNA in the absence and presence of oligomeric and monomeric hSSB1, respectively (as these signals do not overlap with any protein resonances). Notably, significantly larger peak broadening was observed in the case of the hSSB1 oligomer, confirming that large protein oligomers bind to the ssDNA. Given the existence of hSSB1 tetramers in solution as demonstrated earlier (21), it is highly likely that the same tetrameric structures are able to form stable protein-ssDNA complexes.

Oligomeric hSSB1 possesses a distinct ssDNA binding interface
In our previous study, we used HSQC NMR experiments to determine the hSSB1 oligomerisation interface (21). To establish the structural difference in the ssDNA binding mechanism between monomeric and oligomeric hSSB1, we used a similar experimental approach (Figure 5A). Overall, as expected, similar hSSB1 residues exhibit chemical shift changes upon addition of oligo$(dT)_{12}$ ssDNA; however, significantly larger changes were seen for some residues in the case of the oligomeric protein (red bars in Figure 5B), highlighting additional contacts made by the ssDNA in the oligomeric as compared to the monomeric protein structure. We have mapped these residues onto our existing structural model of the hSSB1 tetramer in analogy to Figure 4 (coloured in red in Figures 5C and D). Whereas some of these key residues are located within the known ssDNA binding interface (for the monomeric protein), others (G87, G89 and G90) form part of a distinct patch close to the 5′ ends of the oligo$(dT)_6$ ssDNA (indicated in Figure 5C). However, none are located on the opposite side of the tetrameric protein where the C99-C99 disulphide bond is located (Figure 5D). Interestingly, in the HSQC spectrum of oligomeric hSSB1, the peak for R88 (which is located at the ends of the distinct binding patch) disappears upon addition of ssDNA indicating that this residue plays a major role in the recognition of ssDNA by oligomeric but not monomeric protein.

Oligomeric hSSB1 exhibits different binding kinetics compared to monomeric protein
Having established distinct structural differences in ssDNA binding between oligomeric and monomeric hSSB1, we next sought to corroborate these data by determining the interaction kinetics using surface plasmon resonance (SPR) measurements. As seen in Figure 6, oligomeric $hSSB1_{1\text{-}123}$ recognises oligo$(dT)_{12}$ ssDNA with significantly different binding kinetics (in particular in relation to the off-rate) and a ~7-fold decrease in the dissociation constant compared to the monomeric protein. These data are in good agreement with the NMR data from Figures 4 and 5 and provide further strong evidence that ssDNA binding of oligomeric hSSB1 takes place by direct binding of hSSB1 oligomers (e.g., tetramers) as opposed to successive addition of monomers (under reducing conditions).

Structural models of hSSB1 tetramer-ssDNA complexes
Our hSSB1 tetramer model was initially based on comparisons with the tetramer formed by the OB domains from *E. coli* SSB (EcSSB) (24). Despite the structural similarities between the respective protein tetramers, the actual alignment when forming tetramers is significantly different between the two proteins. The ssDNA binding grooves in the EcSSB tetramer (in the $(EcSSB)_{65}$ binding mode) do

not form a continuous binding surface, and to maintain the same binding polarity the strands of ssDNA wrap around the four monomers (Figure 7A; PDB ID 1EYG).
In contrast, our NMR data (Figures 3 and 5) demonstrate that oligomeric hSSB1 can recognise ssDNA in both binding orientations using a binding interface that is significantly different to EcSSB. In addition, the presence of the C99-C99 disulphide bond in the hSSB1 tetramer presents an obvious obstacle to ssDNA binding in this region and would prevent the ssDNA from interacting with the hSSB1 tetramer in the conformation seen in EcSSB.
Figures 3C,D and Figures 5C,D show one possible structural model of a hSSB1 tetramer-ssDNA complex that is consistent with all the data obtained in this study; a cartoon representation of that model is also shown in Figure 7B (the arrows in panels A-C indicates the position of the C99-C99 disulphide bond in the hSSB1 tetramer). In theory, every hSSB1 monomer can bind ssDNA in both binding orientations as indicated in Figure 7C, increasing the number of possible structural configurations.
In contrast to EcSSB, the DNA recognition regions in hSSB1 monomers align in such a way that one continuous strand of ssDNA (of changing binding polarity) could hypothetically bind across the tetramer. To visualise this structurally, we used our existing disulphide-linked tetramer model (21) in combination with our NMR data (Figures 3 and 5) in the program HADDOCK (25,26) to calculate a structural model of a hSSB1-oligo$(dT)_{12}$ complex. Figure 7D-E depict the lowest-energy structure from a total of 1000 HADDOCK structures representing one hSSB1 tetramer and two oligo$(dT)_{12}$ molecules (termed hSSB1 model (3)). Oligo$(dT)_{12}$ ssDNA recognition on both sides of this tetramer is mediated by two different non disulphide-linked hSSB1 monomers (labelled as I/III and II/IV in Figure 7E, in accordance with reference (21)) and occurs in both binding orientations, in agreement with our PRE data (Figure 3). Notably, in good agreement with our HSQC experiments in Figure 5, extensive contacts between all four R88 residues and the ssDNA are observed in the structural model, confirming that this residue plays an important role in the recognition of ssDNA by hSSB1 tetramers.

Discussion

ssDNA binding mode

We have shown that the ssDNA binding affinity of hSSB1 is strongly dependent on the oligomeric state of the protein (Figure 6), which is determined by oxidative conditions in the nucleus of the cell. In contrast, other important SSBs have been shown to display different binding modalities that correlate with conformational changes vital to their function in ssDNA processing (27-29).
For example, replication protein A (RPA) has varying affinities for ssDNA depending on the different configurations of its components. While hSSB1 contains a single OB domain and forms homo-tetramers (as well as larger oligomers) where each subunit contains a single OB fold, RPA is a heterotrimer that possesses four different ssDNA binding OB domains across two (RPA70 and RPA32) of its three subunits (RPA70, RPA32 and RPA14) and binds ssDNA in three different configurations (30-34). EcSSB on the other hand, binds ssDNA exclusively as a stable homo-tetramer (35-37) with two major binding modes, $(EcSSB)_{65}$ and $(EcSSB)_{35}$, depending on solution conditions. Under high salt conditions, EcSSB adopts the $(EcSSB)_{65}$ binding mode (Figure 7A) where long strands of ssDNA wind through the centre of the tetramer and bind to each of the four subunits simultaneously with the same directionality (37,38).

ssDNA binding polarity

The number and sequence of amino acids present in OB fold-containing proteins varies, however, there are several structural features that are common to all OB folds. OB folds from all three domains of life contain five anti-parallel β strands, coiled to form a β-barrel structure that is capped by an α helix between the third and fourth β strands at one end, and those that bind ssDNA contain a ssDNA binding cleft at the other (39). This ssDNA binding cleft is defined by two loops at the surface of the OB fold, perpendicular to the axis of the β-barrel (23).
Importantly, while the described ssDNA interaction interface is utilised throughout the entire OB domain family of proteins, the orientation that the DNA adopts (DNA binding polarity) is not conserved. However, the majority of OB fold proteins recognise ssDNA in what is defined by Theobald et al., (23) as the 'standard binding polarity' in which the DNA binds within the ssDNA binding cleft, with a polarity of 5′ to 3′ from strands β4 and β5 to strand β2 (23). One of two notable

exceptions is the β subunit of *Oxytricha nova* telomere end binding protein (OnTEBP; PDB ID 1K8G) (40), which binds to ssDNA in the reverse orientation ('reverse polarity') (23). The second exception described by Theobald et al. (23) is EcSSB, bound to ssDNA in the $(EcSSB)_{65}$ mode (PDB 1EYG).
Intriguingly, another stable homo-tetramer, the SSB from *Plasmodium falciparum* (PfSSB; PDB ID 3ULP) binds ssDNA adopting a topology that is highly similar to $(EcSSB)_{65}$, however it does so using the standard polarity (41). In contrast, a more recently solved tetrameric OB fold-containing protein structure from *Bacillus subtilis* SsbA (BsSsbA; PDB ID 6BHX) (42) revealed ssDNA binding in the reverse polarity in analogy to EcSSB. These discrepancies could at least partly be explained by crystallographic artefacts in that one ssDNA binding orientation is more stable and therefore crystallised. However, this does not exclude the possibility that structures containing ssDNA with the opposite, or even both binding polarities at the same time, exist *in vivo*. Indeed, the latter is the case in one recently published structure, the tetrameric SSB from *Pseudomonas aeruginosa* (PaSSB; PDB ID 6IRQ; (43)) (Figure 8). Similar to our hSSB1-ssDNA complex model (Figure 7D-E), in this crystal structure both ssDNA binding directionalities are observed, however, the ssDNA exists as two separate strands as the alignment of the ssDNA binding grooves is significantly different to hSSB1.
Orientation of ssDNA binding plays an important functional role for some SSBs, as is the case for human RPA in the context of nucleotide excision repair, where binding polarity appears to be crucial for positioning of the excision repair nucleases XPG and ERCC1-XPF onto the ssDNA (44). However, this contrasts with hSSB1 which forms oligomers as part of the response to oxidative damage. The main function of hSSB1 tetramers is to bind to oxoG lesions that exist in double-stranded DNA, a process that is then followed by the recruitment of hOGG1 that removes the lesion (16,19). As shown in Figure 1, oligomeric hSSB1 is able to open up dsDNA that contains an oxoG base and bind to both single strands, which could technically be achieved as demonstrated in our NMR-based structural model in which both ssDNA binding polarities are observed in the same structure (Figure 7D-E).

Interactions with INTS3
We have previously shown that hSSB1 tetramer formation does not inhibit interaction with Integrator Complex Subunit 3 (INTS3), as two distinct interaction surfaces are utilised for binding (21). Structural models of tetrameric hSSB1-ssDNA complexes based on our NMR and SPR data (Figure 7) reveal that ssDNA binding is mediated by hSSB1 residues that do not form part of the INTS3 recognition surface, thus enabling hSSB1 tetramer binding of INTS3 and ssDNA at the same time.
We have combined one of our structural models (Figure 7D-E) with published data on the INTS binding interface (18) in Figure 9 to show how tetrameric hSSB1 can recognise up to two INTS3 molecules for each hSSB1 tetramer while bound to ssDNA at the same time. Figure 9 shows one out of four possible hSSB1-$INTS3_2$ binding conformations.
Notably, our structural model differs from a model described in a recently deposited preprint (Figure 6 in reference (45)) incorporating hSSB1, ssDNA, INT3, and INTS6. However, in contrast to our model and published data (18), this model (45) reveals direct contacts between the N-terminus of INTS3 and ssDNA. Further structural and biophysical studies will be required to shed light on the exact composition and structural details of the entire SOSS1 complex, comprising hSSB1 (SOSSB1), ssDNA, INTS3 (SOSSA), C9orf80 (SOSSC) and INTS6.

Experimental Procedures
Protein expression and purification
Expression of GST-tagged hSSB1 (residues 1-123 encompassing the OB domain) was induced in *E. coli* BL21(DE3) by the addition of 0.2 mM IPTG for 15 h at 25ºC (20). Isotopically labelled ^{15}N-$hSSB1_{1-123}$ was prepared in a fermenter to allow for nitrogen levels to be monitored and the source of nitrogen to be changed to $^{15}NH_4Cl$ before expression was induced. Cells were lysed by sonication in lysis buffer (10 mM MES, pH 6.0, 50 mM NaCl, 0.5 mM PMSF, 0.1% Triton X 100 (+ 3 mM TCEP for monomeric hSSB1)). Lysed cells were centrifuged, and the supernatant was subjected to GSH affinity chromatography followed by HRV-3C protease cleavage, leaving a five residue (GPLGS) non-native overhang at the N-terminus. Eluate from GSH affinity chromatography was subjected to heparin affinity chromatography using a HiTrap HP Heparin column (5 mL GE Healthcare)

equilibrated with NMR buffer (10 mM MES, pH 6.0, 50 mM NaCl (+ 3 mM TCEP for monomeric hSSB1)). The hSSB1 protein was eluted from the column by increasing salt concentration (50-1000 mM NaCl gradient). Fractions correlating to a distinct peak in UV absorbance (280 nm) were collected and analysed by SDS-PAGE. For SPR, the protein was buffer exchanged into SPR buffer (50 mM Tris, pH 7.6, 50 mM NaCl, 0.4 mM EDTA, 0.005% P20 (+ 0.5 mM DTT for monomeric hSSB1)). Protein concentrations were determined using the absorbance at 280 nm and the theoretical molar extinction coefficient for $hSSB1_{1-123}$ (11460 $M^{-1}cm^{-1}$). Note that protein concentrations refer to the concentration of hSSB1 monomers, in this study.

NMR spectroscopy

Purified protein samples (80-300 µM) were prepared in NMR buffer with 10% deuterium oxide (D_2O) and 20 µM 4,4-dimethyl-4-silapentane-1-sulfonic acid (DSS). One dimensional (1D) and two dimensional (2D) spectra were acquired on a Bruker Avance 600 or 800 MHz spectrometer at 25ºC using standard 1D and 2D pulse programs, respectively. All spectra were processed using TOPSPIN (Bruker, Biospin) with reference to the chemical shift of DSS (0 ppm) and assignments from our previous studies (20,21) were transferred using Sparky (T. D. Goddard and D.G. Kneller, University of California at San Francisco). The calculation of weighted chemical shift changes was carried out as described (46) using OriginPro 2019 (OriginLab Corporation, Northampton, MA, USA). A 38mer dsDNA containing a central 8-oxoG (8-oxoG dsDNA) [5′-CCAGGCTTA(8-oxoG)CTCTTTATG-3′] was made by annealing corresponding single strands of DNA, purified by size exclusion chromatography (superdex 75) and subjected to 1D ^1H NMR and 2D ^1H-^1H NOESY NMR experiments in NMR buffer. Resonances of imino protons (12-14.5 ppm) were assigned using the NOESY spectrum. All ssDNA oligomers were dissolved in NMR buffer prior to recording NMR experiments.

Paramagnetic relaxation enhancement (PRE) labelling

Paramagnetic relaxation enhancement (PRE) NMR techniques using paramagnetic-labelled oligonucleotides (PRE-oligo$(dT)_6$) [5′-G'(PRE)'GTTTTTT-3′] were utilised to determine the orientation in which ssDNA binds to hSSB1. Synthesis and purification of the PRE-labelled ssDNA was carried out in analogy to the study on the SSB from *Sulfolobus solfataricus* (SsoSSB) (22). However, in contrast to the described method (22), a reduced version of the paramagnetic-labelled oligonucleotide could not be used in this study due to the reducing agent impacting on the oligomeric state of the hSSB1 protein. Thus, an unlabelled oligonucleotide [5′-G'GTTTTTT-3′] was used as a control. Both PRE- and control ssDNAs were prepared in NMR buffer. The ratio of the peak intensities of hSSB1 bound to control DNA versus PRE-labelled DNA from HSQC spectra were calculated using Sparky (T. D. Goddard and D.G. Kneller, University of California at San Francisco) and plotted in OriginPro 2019 (OriginLab Corporation, Northampton, MA, USA).

Surface Plasmon Resonance (SPR)

All SPR experiments were carried out on a BIAcore T200, utilising the biotin-streptavidin system. Biotinylated oligo$(dT)_{12}$ ssDNA with a 3A spacer [5′-btn-AAATTTTTTTTTTTTT-3′] was injected into flow cell 2 of a streptavidin coated sensor (SA) chip at a flow rate of 5 µL/min for 190 s in SPR buffer. Approximately 88 response units (RU) of DNA was immobilised onto the surface. An unmodified flow cell 1 acted as a control. Solutions of purified $hSSB1_{1-123}$ were injected for 20 s (monomer) or 1000 s (oligomer) at a flow rate of 20 µL/min. Flow cells were regenerated with 1 min injections of 1M $MgCl_2$ (monomer) and 2 min injections of 2 M $MgCl_2$ (oligomer) at 5 µL/min. Data obtained from SPR experiments were analysed using BIAevaluation 4.1.1. Regions chosen to determine equilibrium values were selected at the point of saturation. The dissociation constant (K_D) and the theoretical response for binding of analyte at saturation to immobilised ligands (R_{max}) of each interaction was derived from the correlation between the equilibrium values of the binding curve, and the $hSSB1_{1-123}$ concentration by fitting data to the Langmuir equation. All SPR figures were created using OriginPro 2019 (OriginLab Corporation, Northampton, MA, USA) and edited using Adobe Illustrator 2020.24.2.

HADDOCK modelling

The hSSB1 tetramer model as published by Touma et al. 2017 (21) was modelled together with ssDNA (oligo$(dT)_{12}$) using the same restraints as previously used (20). hSSB1 residues 15–17, 26–40, 52–63 and 73–91 were defined as semi-flexible and all twelve thymidines of the ssDNA were defined as semi-flexible and flexible. A total of 83 ambiguous interaction restraints (AIRs) based on (20) and 28 unambiguous interaction restraints (UIRs) based on (21) between each hSSB1 monomer and ssDNA were selected and fixed at 2 Å. Additional restraints to maintain base planarity between the four aromatic residues (W55, Y74, F78 and Y85) and ssDNA bases THY2, THY3, THY5, THY8, THY10 and THY11 as well as the overall symmetry of the hSSB1 oligomer were used in the calculations. The conformer with the lowest value of total energy of the lowest-energy cluster (out of 1000 calculated structures) was analysed and visualised using PYMOL (Schrödinger, NY).

Acknowledgements
We would like to thank Dr Ann Kwan for expert maintenance of the NMR spectrometers and Prof Nicholas Dixon for critical reading of the manuscript.

Conflict of interest
The authors declare that they have no conflicts of interest with the contents of this article.

References
1. Kryston, T. B., Georgiev, A. B., Pissis, P., and Georgakilas, A. G. (2011) Role of oxidative stress and DNA damage in human carcinogenesis. *Mutation research* **711**, 193-201
2. Olinski, R., Gackowski, D., Foksinski, M., Rozalski, R., Roszkowski, K., and Jaruga, P. (2002) Oxidative DNA damage: assessment of the role in carcinogenesis, atherosclerosis, and acquired immunodeficiency syndrome1. *Free Radical Biology and Medicine* **33**, 192-200
3. Maynard, S., Schurman, S. H., Harboe, C., de Souza-Pinto, N. C., and Bohr, V. A. (2009) Base excision repair of oxidative DNA damage and association with cancer and aging. *Carcinogenesis* **30**, 2-10
4. Nakabeppu, Y. (2014) Cellular levels of 8-oxoguanine in either DNA or the nucleotide pool play pivotal roles in carcinogenesis and survival of cancer cells. *Int J Mol Sci* **15**, 12543-12557
5. Loft, S., and Poulsen, H. (1996) Cancer risk and oxidative DNA damage in man. *Journal of Molecular Medicine* **74**, 297-312
6. Wilson, D. M., 3rd, and Bohr, V. A. (2007) The mechanics of base excision repair, and its relationship to aging and disease. *DNA Repair (Amst)* **6**, 544-559
7. Olinski, R. (2003) Oxidative DNA damage in cancer patients: a cause or a consequence of the disease development? *Mutation Research/Fundamental and Molecular Mechanisms of Mutagenesis* **531**, 177-190
8. David, S. S., O'Shea, V. L., and Kundu, S. (2007) Base-excision repair of oxidative DNA damage. *Nature* **447**, 941-950
9. Krokan, H. E., and Bjoras, M. (2013) Base excision repair. *Cold Spring Harbor perspectives in biology* **5**, a012583
10. Scott, T. L., Rangaswamy, S., Wicker, C. A., and Izumi, T. (2014) Repair of oxidative DNA damage and cancer: recent progress in DNA base excision repair. *Antioxidants & redox signaling* **20**, 708-726
11. Croft, L. V., Bolderson, E., Adams, M. N., El-Kamand, S., Kariawasam, R., Cubeddu, L., Gamsjaeger, R., and Richard, D. J. (2018) Human single-stranded DNA binding protein 1 (hSSB1, OBFC2B), a critical component of the DNA damage response. *Semin Cell Dev Biol* **86**, 121-128
12. Flynn, R. L., and Zou, L. (2010) Oligonucleotide/oligosaccharide-binding fold proteins: a growing family of genome guardians. *Crit Rev Biochem Mol Biol* **45**
13. Richard, D. J., Cubeddu, L., Urquhart, A. J., Bain, A., Bolderson, E., Menon, D., White, M. F., and Khanna, K. K. (2011) hSSB1 interacts directly with the MRN complex stimulating its recruitment to DNA double-strand breaks and its endo-nuclease activity. *Nucleic acids research* **39**, 3643-3651
14. Richard, D. J., Savage, K., Bolderson, E., Cubeddu, L., So, S., Ghita, M., Chen, D. J., White, M. F., Richard, K., Prise, K. M., Schettino, G., and Khanna, K. K. (2011) hSSB1 rapidly binds at the

sites of DNA double-strand breaks and is required for the efficient recruitment of the MRN complex. *Nucleic acids research* **39**, 1692-1702
15. Skaar, J. R., Richard, D. J., Saraf, A., Toschi, A., Bolderson, E., Florens, L., Washburn, M. P., Khanna, K. K., and Pagano, M. (2009) INTS3 controls the hSSB1-mediated DNA damage response. *The Journal of cell biology* **187**, 25-32
16. Paquet, N., Adams, M. N., Leong, V., Ashton, N. W., Touma, C., Gamsjaeger, R., Cubeddu, L., Beard, S., Burgess, J. T., Bolderson, E., O'Byrne, K. J., and Richard, D. J. (2015) hSSB1 (NABP2/ OBFC2B) is required for the repair of 8-oxo-guanine by the hOGG1-mediated base excision repair pathway. *Nucleic acids research* **43**, 8817-8829
17. Ashton, N. W., Bolderson, E., Cubeddu, L., O'Byrne, K. J., and Richard, D. J. (2013) Human single-stranded DNA binding proteins are essential for maintaining genomic stability. *BMC Molecular Biology* **14**, 9
18. Ren, W., Chen, H., Sun, Q., Tang, X., Lim, S. C., Huang, J., and Song, H. (2014) Structural basis of SOSS1 complex assembly and recognition of ssDNA. *Cell reports* **6**, 982-991
19. Paquet, N., Adams, M. N., Ashton, N. W., Touma, C., Gamsjaeger, R., Cubeddu, L., Leong, V., Beard, S., Bolderson, E., Botting, C. H., O'Byrne, K. J., and Richard, D. J. (2016) hSSB1 (NABP2/OBFC2B) is regulated by oxidative stress. *Scientific reports* **6**, 27446
20. Touma, C., Kariawasam, R., Gimenez, A. X., Bernardo, R. E., Ashton, N. W., Adams, M. N., Paquet, N., Croll, T. I., O'Byrne, K. J., Richard, D. J., Cubeddu, L., and Gamsjaeger, R. (2016) A structural analysis of DNA binding by hSSB1 (NABP2/OBFC2B) in solution. *Nucleic acids research* **44**, 7963-7973
21. Touma, C., Adams, M. N., Ashton, N. W., Mizzi, M., El-Kamand, S., Richard, D. J., Cubeddu, L., and Gamsjaeger, R. (2017) A data-driven structural model of hSSB1 (NABP2/OBFC2B) self-oligomerization. *Nucleic acids research* **45**, 8609-8620
22. Gamsjaeger, R., Kariawasam, R., Gimenez, Adrian X., Touma, C., McIlwain, E., Bernardo, Ray E., Shepherd, Nicholas E., Ataide, Sandro F., Dong, Q., Richard, Derek J., White, Malcolm F., and Cubeddu, L. (2015) The structural basis of DNA binding by the single-stranded DNA-binding protein from Sulfolobus solfataricus. *Biochemical Journal* **465**, 337-346
23. Theobald, D. L., Mitton-Fry, R. M., and Wuttke, D. S. (2003) Nucleic acid recognition by OB-fold proteins. *Annu Rev Biophys Biomol Struct* **32**, 115-133
24. Savvides, S. N., Raghunathan, S., Futterer, K., Kozlov, A. G., Lohman, T. M., and Waksman, G. (2004) The C-terminal domain of full-length E. coli SSB is disordered even when bound to DNA. *Protein Sci* **13**, 1942-1947
25. Dominguez, C., Boelens, R., and Bonvin, A. M. (2003) HADDOCK: a protein-protein docking approach based on biochemical or biophysical information. *J Am Chem Soc* **125**, 1731-1737
26. van Zundert, G. C. P., Rodrigues, J., Trellet, M., Schmitz, C., Kastritis, P. L., Karaca, E., Melquiond, A. S. J., van Dijk, M., de Vries, S. J., and Bonvin, A. (2016) The HADDOCK2.2 Web Server: User-Friendly Integrative Modeling of Biomolecular Complexes. *J Mol Biol* **428**, 720-725
27. Shereda, R. D., Kozlov, A. G., Lohman, T. M., Cox, M. M., and Keck, J. L. (2008) SSB as an organizer/mobilizer of genome maintenance complexes. *Critical reviews in biochemistry and molecular biology* **43**, 289-318
28. Brosey, C. A., Yan, C., Tsutakawa, S. E., Heller, W. T., Rambo, R. P., Tainer, J. A., Ivanov, I., and Chazin, W. J. (2013) A new structural framework for integrating replication protein A into DNA processing machinery. *Nucleic acids research* **41**, 2313-2327
29. Fanning, E., Klimovich, V., and Nager, A. R. (2006) A dynamic model for replication protein A (RPA) function in DNA processing pathways. *Nucleic acids research* **34**, 4126-4137
30. Bastin-Shanower, S. A., and Brill, S. J. (2001) Functional analysis of the four DNA binding domains of Replication Protein A: the role of RPA2 in ssDNA binding. *The Journal of biological chemistry* **276**, 36446-36453
31. Bochkarev, A., A. Pfuetzner, R., M. Edwards, A., and Frappier, L. (1997) *Structure of the single-stranded-DNA-binding domain of replication protein A bound to DNA*,
32. Cai, L., Roginskaya, M., Qu, Y., Yang, Z., Xu, Y., and Zou, Y. (2007) A Structural Characterization of Human RPA Sequential Binding to Single-Stranded DNA Using ssDNA as a Molecular Ruler. *Biochemistry* **46**, 8226-8233

33. Fan, J., and Pavletich, N. P. (2012) Structure and conformational change of a replication protein A heterotrimer bound to ssDNA. *Genes & Development* **26**, 2337-2347
34. Salas, T. R., Petruseva, I., Lavrik, O., and Saintomé, C. (2009) Evidence for direct contact between the RPA3 subunit of the human replication protein A and single-stranded DNA. *Nucleic acids research* **37**, 38-46
35. Lohman TM, and ME, F. (1994) Escherichia Coli Single-Stranded DNA-Binding Protein: Multiple DNA-Binding Modes and Cooperativities. *Annual Review of Biochemistry* **63**, 527-570
36. Raghunathan, S., Ricard, C. S., Lohman, T. M., and Waksman, G. (1997) Crystal structure of the homo-tetrameric DNA binding domain of Escherichia coli single-stranded DNA-binding protein determined by multiwavelength x-ray diffraction on the selenomethionyl protein at 2.9-Å resolution. *Proceedings of the National Academy of Sciences* **94**, 6652-6657
37. Raghunathan, S., Kozlov, A. G., Lohman, T. M., and Waksman, G. (2000) Structure of the DNA binding domain of E. coli SSB bound to ssDNA. *Nature Structural Biology* **7**, 648
38. Roy, R., Kozlov, A. G., Lohman, T. M., and Ha, T. (2007) Dynamic Structural Rearrangements Between DNA Binding Modes of E. coli SSB Protein. *Journal of Molecular Biology* **369**, 1244-1257
39. Murzin, A. (1993) OB(oligonucleotide/oligosaccharide binding)-fold: common structural and functional solution for non-homologous sequences. *The EMBO Journal* **12**, 861-867
40. Classen, S., Ruggles, J. A., and Schultz, S. C. (2001) Crystal structure of the N-terminal domain of Oxytricha nova telomere end-binding protein alpha subunit both uncomplexed and complexed with telomeric ssDNA. *J Mol Biol* **314**, 1113-1125
41. Antony, E., Weiland, E. A., Korolev, S., and Lohman, T. M. (2012) Plasmodium falciparum SSB Tetramer Wraps Single-Stranded DNA with Similar Topology but Opposite Polarity to E. coli SSB. *Journal of Molecular Biology* **420**, 269-283
42. Dubiel, K., Myers, A. R., Kozlov, A. G., Yang, O., Zhang, J., Ha, T., Lohman, T. M., and Keck, J. L. (2019) Structural Mechanisms of Cooperative DNA Binding by Bacterial Single-Stranded DNA-Binding Proteins. *J Mol Biol* **431**, 178-195
43. Huang, Y.-H., Chen, I. C., and Huang, C.-Y. (2019) Characterization of an SSB–dT25 complex: structural insights into the S-shaped ssDNA binding conformation. *RSC Advances* **9**, 40388-40396
44. de Laat, W. L., Appeldoorn, E., Sugasawa, K., Weterings, E., Jaspers, N. G., and Hoeijmakers, J. H. (1998) DNA-binding polarity of human replication protein A positions nucleases in nucleotide excision repair. *Genes Dev* **12**, 2598-2609
45. Jia, Y., Cheng, Z., Bharath, S. B., Sun, Q., Su, N., Huang, J., and Song, H. (2020) Crystal Structure of INTS3/INTS6 complex reveals Functional Importance of INTS3 dimerization in DSB Repair. *bioRxiv DOI: 10.1101/2020.04.10.035014*
46. Ayed, A., Mulder, F. A. A., Yi, G.-S., Lu, Y., Kay, L. E., and Arrowsmith, C. H. (2001) Latent and active p53 are identical in conformation. *Nature Structural Biology* **8**, 756

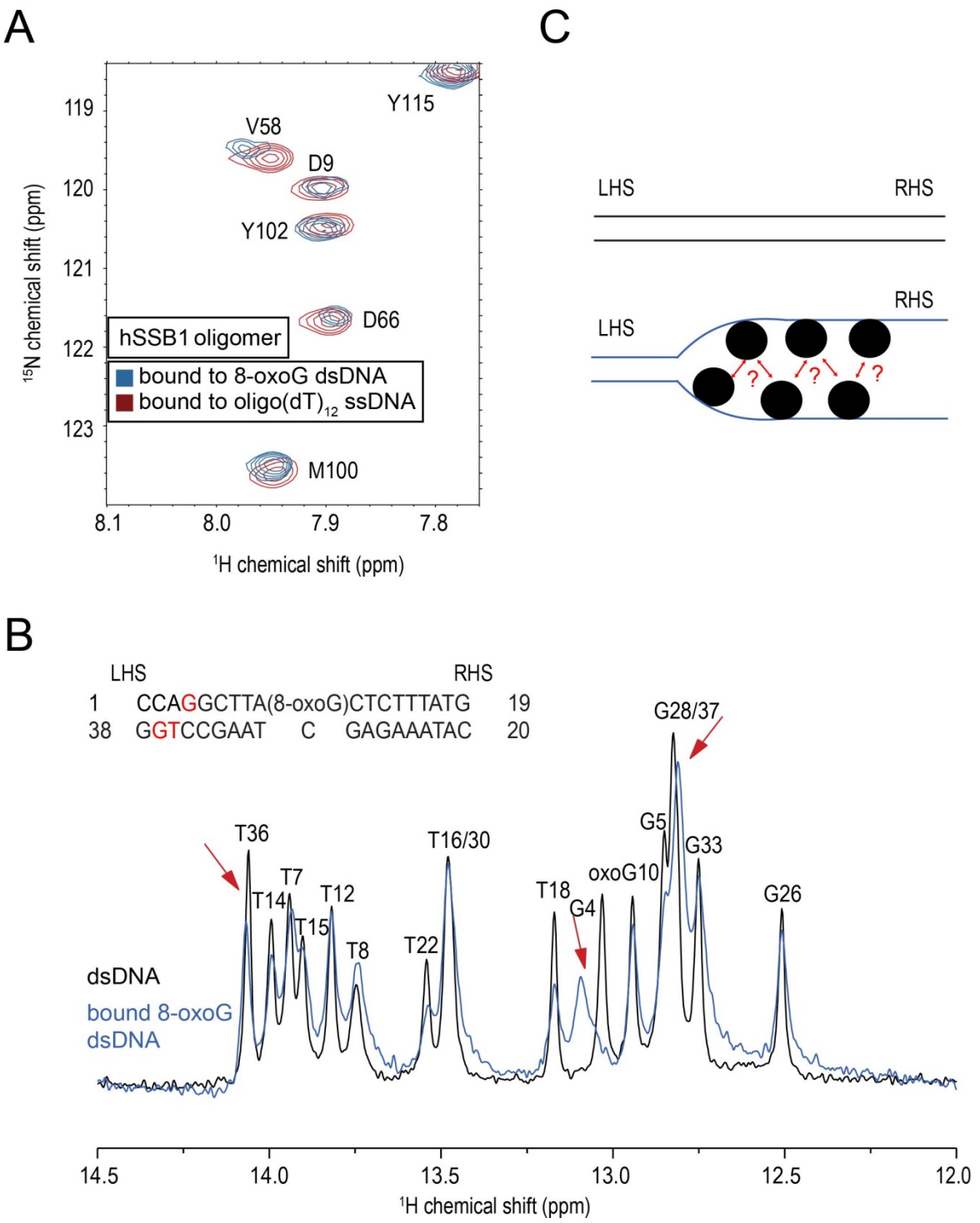

Figure 1. Oligomeric hSSB1 binding to 8-oxoG containing dsDNA. A. Portion of assigned ^{15}N HSQC spectra of hSSB1$_{1\text{-}123}$ bound to 8-oxoG dsDNA (1:1; red) and oligo(dT)$_{12}$ ssDNA (1:1; blue), respectively. **B.** 1D ^{1}H NMR spectrum showing imino protons (indicative of Watson-Crick bonds in double-stranded DNA) of dsDNA containing an oxoG nucleotide in the absence (black) and presence (blue) of oligomeric hSSB1$_{1\text{-}123}$. The dsDNA sequence is shown as an inset in the top left. DNA bases of intact dsDNA molecules whose resonances were seen to shift upon addition of oligomeric hSSB1$_{1\text{-}123}$ are indicated by red arrows (coloured in red in the sequence). **C.** Schematic of dsDNA binding by oligomeric hSSB1.

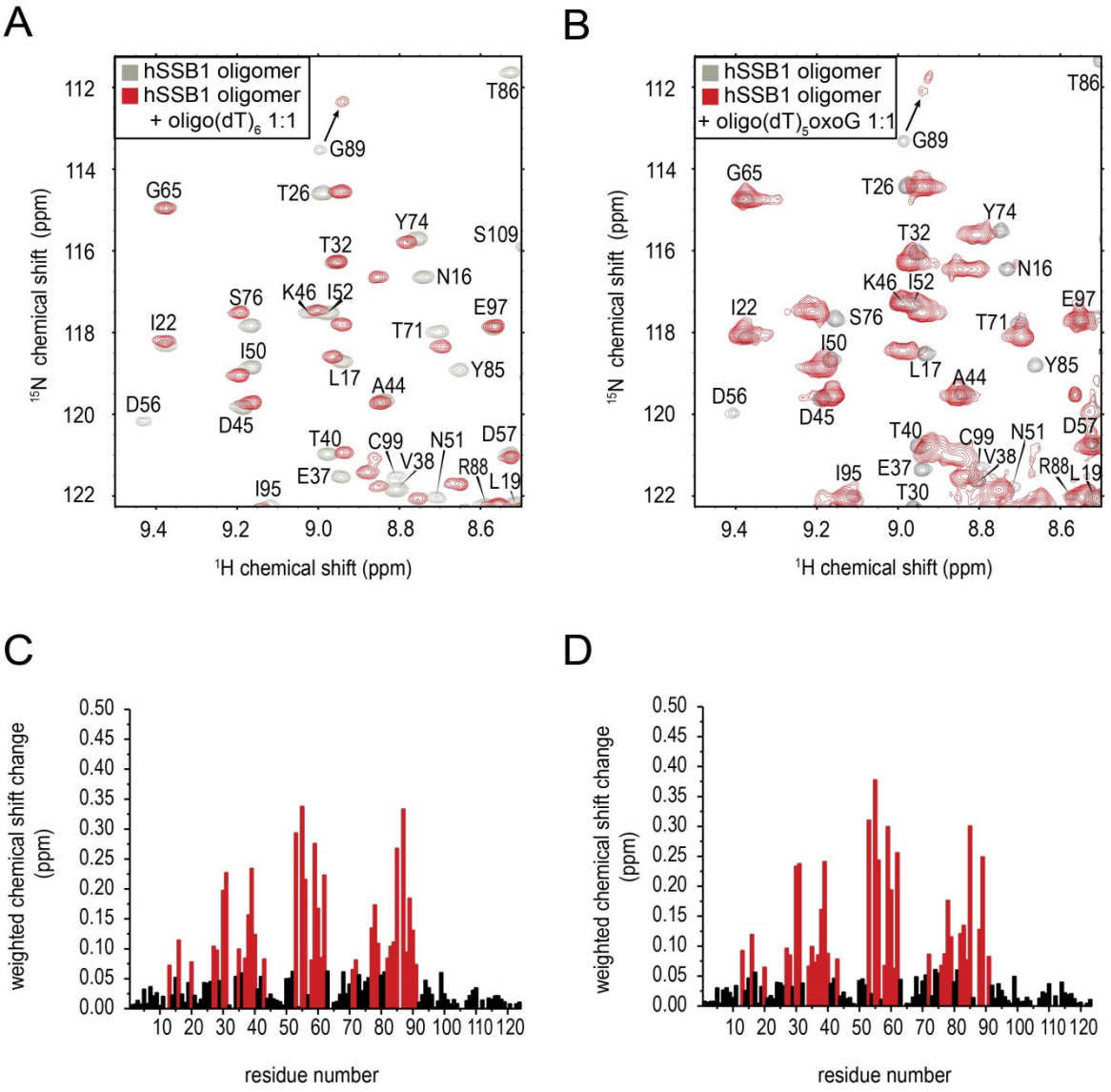

Figure 2. Oligomeric hSSB1 binding to 8-oxoG containing ssDNA. Section of ^{15}N HSQC spectra of oligomeric hSSB1$_{1-123}$ in the absence (1:1; grey) and presence (1:1; red) of oligo(dT)$_6$ ssDNA (5′-TTTTTT-3′) (**A**) and 5ToxoG ssDNA (5′-TT(8-oxoG)TTT-3′) (**B**), respectively. **C-D.** Weighted backbone chemical shift changes of HN and N (46) atoms for hSSB1$_{1-123}$ upon binding to oligo(dT)$_6$ (**C**) and 5ToxoG (**D**) ssDNA, respectively. Residues that exhibit higher than average chemical shift changes are highlighted in red. Note the similarity of the chemical shift profiles of panels C and D.

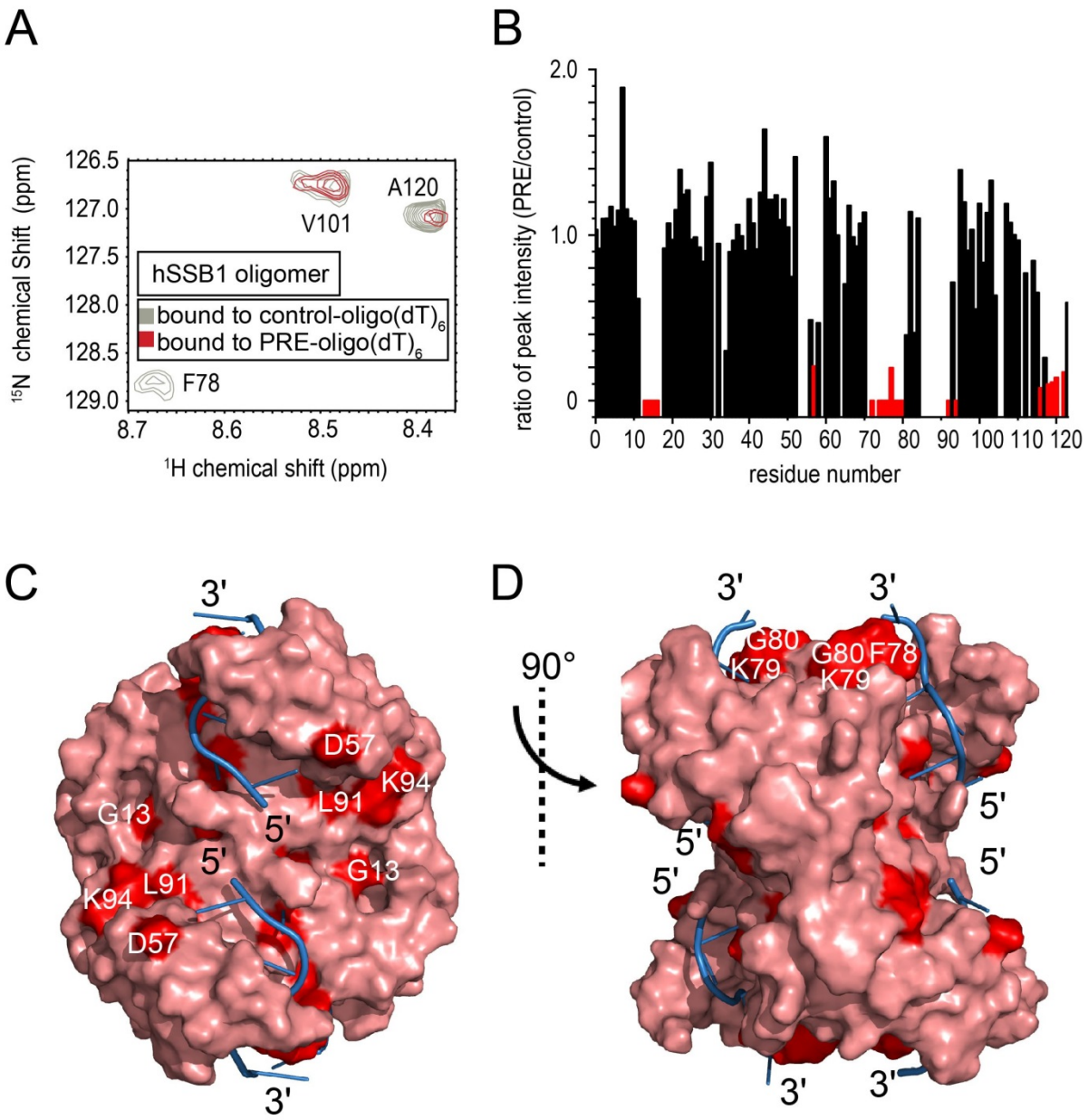

Figure 3. PRE analysis of oligomeric hSSB1 binding to ssDNA. A. Section of ^{15}N HSQC spectra of a 1:1 mixture of hSSB1$_{1\text{-}123}$ with paramagnetic nitroxide spin-labelled ssDNA [5′-G'(PRE)'GTTTTTT-3′] (PRE-oligo(dT)$_6$; red) and diamagnetic non-labelled ssDNA [5′-G'GTTTTTT-3′] (control-oligo(dT)$_6$; grey). Note that signals originating from residues that are close to the paramagnetic centre either disappear or are significantly reduced under paramagnetic conditions. **B.** Ratio of HSQC peak intensities of hSSB1$_{1\text{-}123}$ residues under paramagnetic (PRE-oligo(dT)$_6$) versus diamagnetic (control-oligo(dT)$_6$) conditions. Ratios from signals of residues that exhibit a decrease significantly smaller (average minus two times standard deviation) than the average ratio or disappear entirely (ratio equals zero) are indicated in red in panel B. These residues were mapped onto the published hSSB1 tetramer model (red) with the oligo(dT)$_6$ ssDNA from the monomeric protein present (taken from (20) (**C-D**). Note that affected residues are located close to both the 3′ and the 5′ end of the ssDNA.

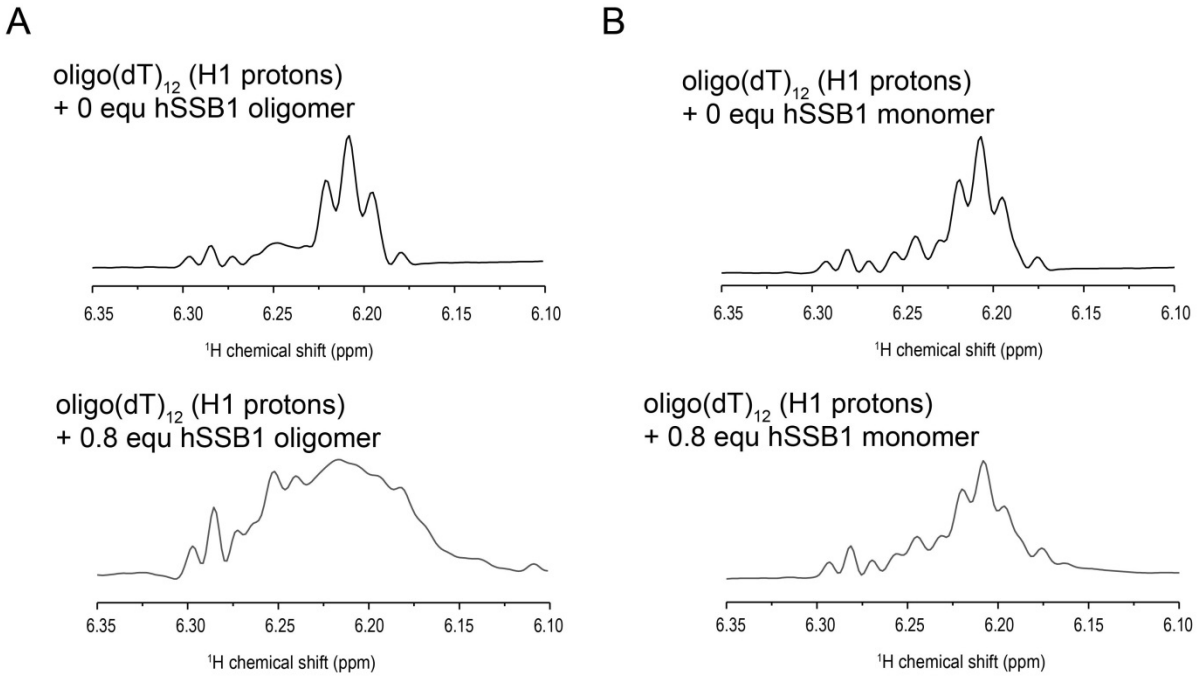

Figure 4. Difference of oligomeric versus monomeric hSSB1 binding to oligo(dT)$_{12}$ ssDNA by 1D NMR experiments. Section of 1D ^{1}H spectra of oligo(dT)$_{12}$ ssDNA showing H1 sugar protons in the absence (top) and presence (bottom) of oligomeric hSSB1$_{1\text{-}123}$ (**A**) or monomeric hSSB1$_{1\text{-}123}$ (**B**), respectively.

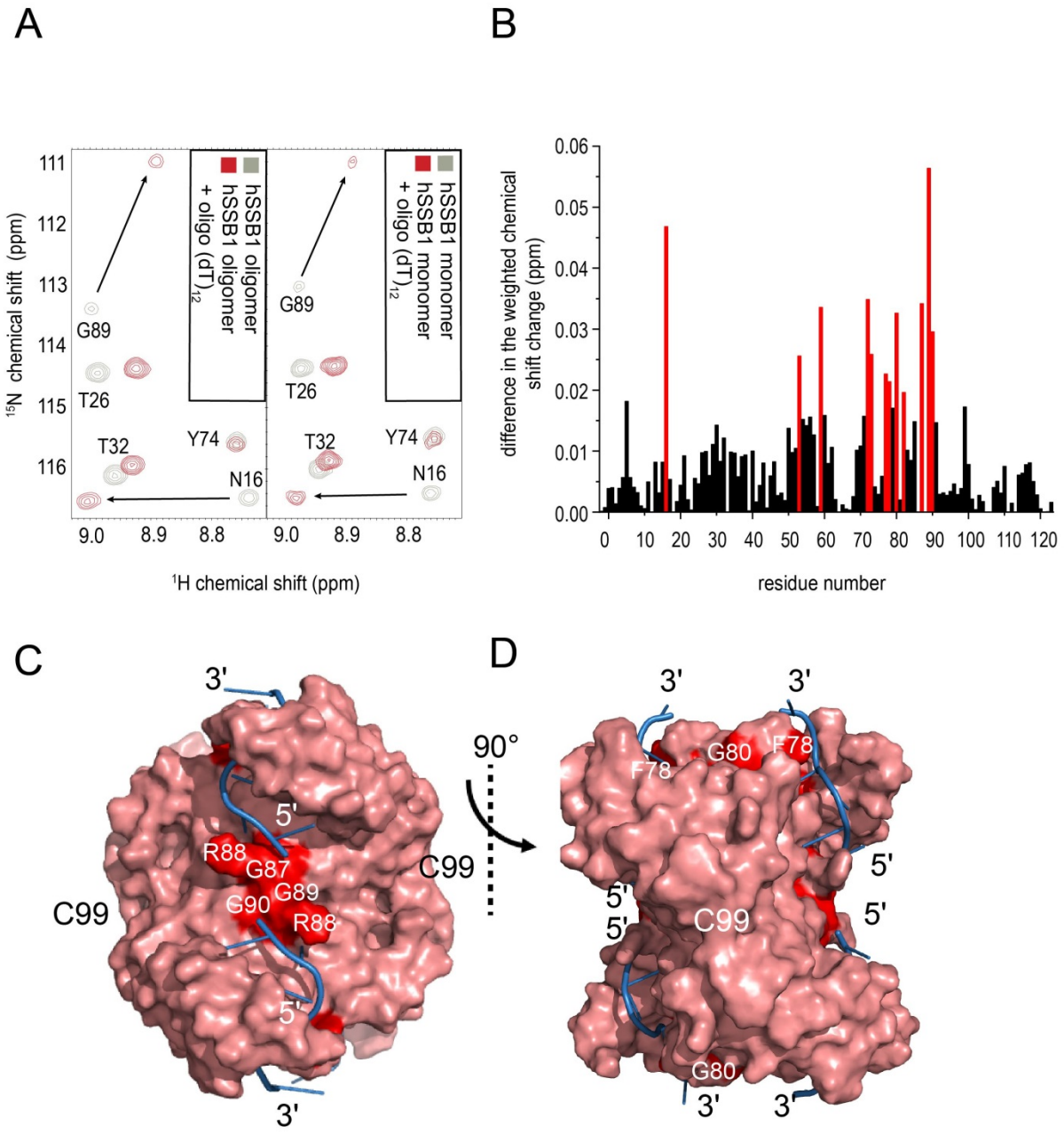

Figure 5. Difference of oligomeric versus monomeric hSSB1 binding to oligo(dT)$_{12}$ ssDNA by 2D NMR HSQC experiments. A. Portion of ^{15}N HSQC spectra of a 1:1 mixture of oligo(dT)$_{12}$ ssDNA with oligomeric (left-hand side) or monomeric (right-hand side) hSSB1$_{1\text{-}123}$, respectively. **B.** Difference in the weighted chemical shift changes between oligomeric and monomeric proteins. Residues exhibiting differences in changes that are significantly higher than average are highlighted as red bars. These residues were mapped onto our tetramer model with the oligo(dT)$_6$ ssDNA taken from (20) present (**C-D**). The surface representation in panel C is depicted in the same orientation as in Figure 3C. A distinct binding patch (comprising residues G87, R88, G89 and G90) that is located between the 5′ ends of the oligo(dT)$_6$ ssDNA is coloured in red. The position of the disulphide bonds between C99 residues is indicated.

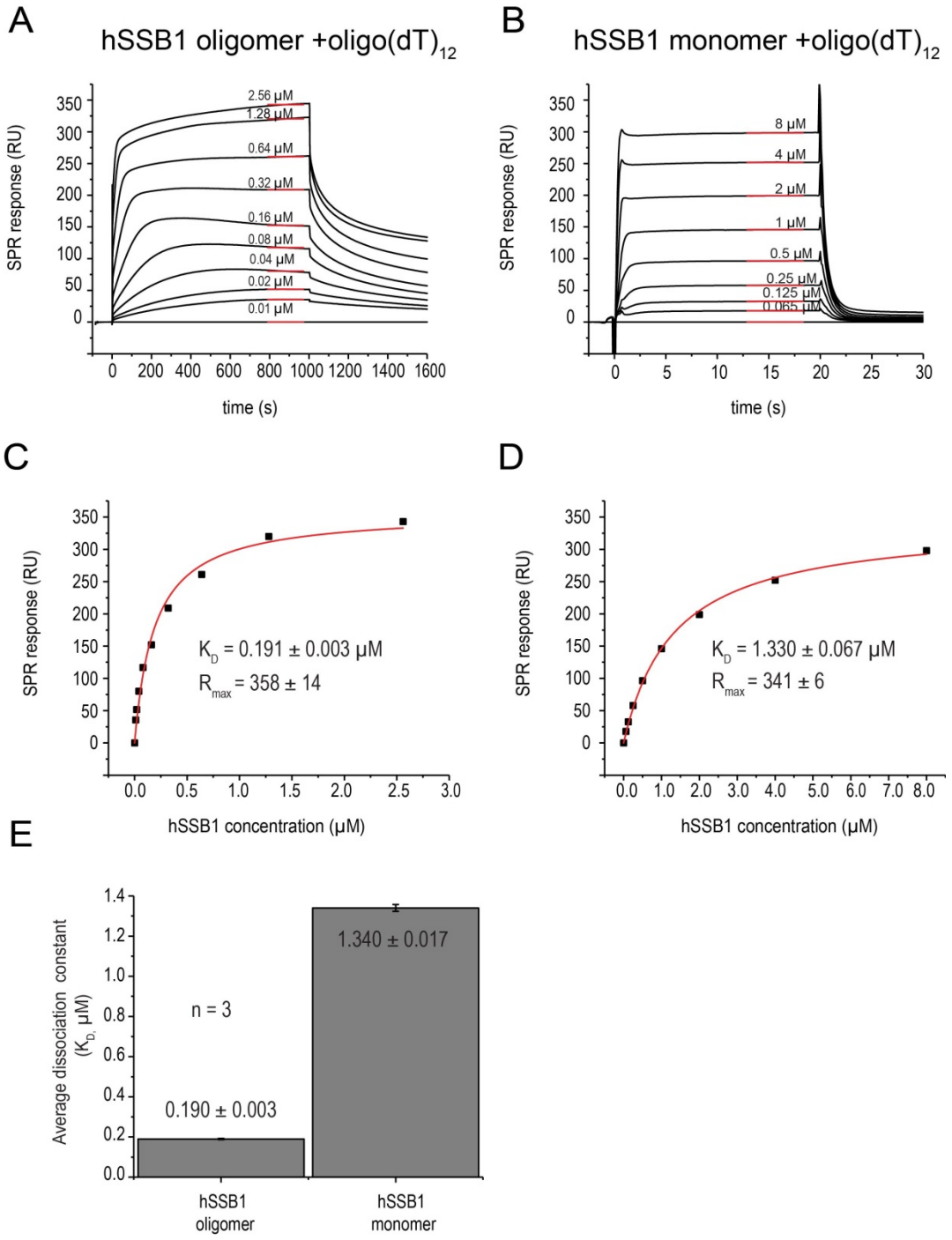

Figure 6. SPR analysis of binding of oligomeric hSSB1 to oligo(dT)$_{12}$ ssDNA. Representative SPR binding curves of interaction between oligomeric (**A**) and monomeric hSSB1$_{1-123}$ (**B**), respectively (concentration relates to monomers; note the different timescales used for data collection), with oligo(dT)$_{12}$ ssDNA. **C-D.** Equilibrium values (as indicated by the red lines in panels A and B) for both oligomeric and monomeric proteins were plotted against the hSSB1$_{1-123}$ concentration and fitted to the Langmuir equation (steady-state analysis). **E.** Dissociation constants were calculated from three independent experiments for both oligomeric and monomeric protein.

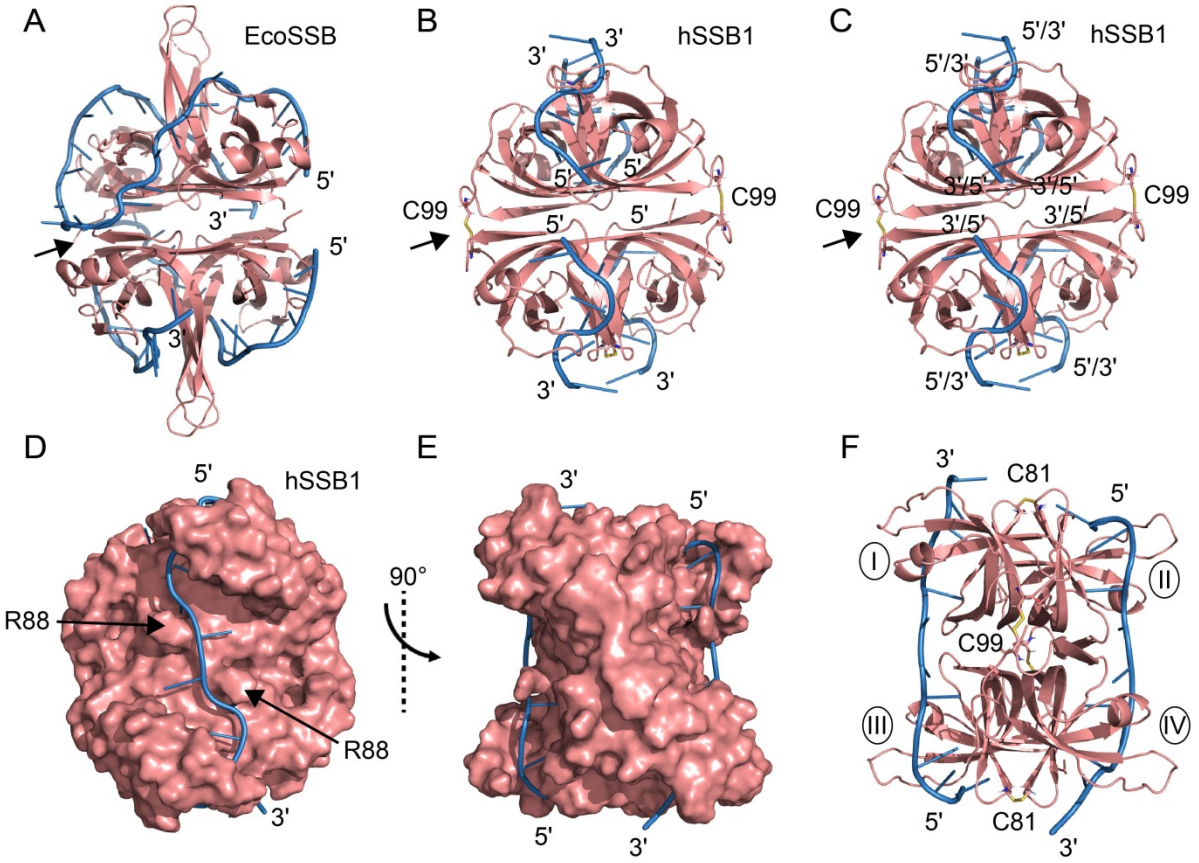

Figure 7. Structural models of hSSB1 tetramers bound to ssDNA. A. Crystal structure of the EcSSB tetramer (salmon) bound to ssDNA (blue) (PDB ID 1EYG) (24). **B.** Structural model of the hSSB1 tetramer (salmon) taken from (21) with the oligo$(dT)_6$ ssDNA (blue) overlaid from the ssDNA bound monomeric structure published in (20). **C.** Same model as in B with all possible ssDNA binding polarities indicated. The disulphide bond between C99 is indicated in panels B and C. Note the difference in alignment of the ssDNA binding grooves between EcSSB and hSSB1. Surface (**D-E**) as well as cartoon (**F**) representation of a structural model of a hSSB1-oligo$(dT)_{12}$ complex (hSSB1 complex (3); protein coloured in salmon, ssDNA shown in blue) calculated by the program HADDOCK (25,26). The essential binding residue R88 for two protein monomers is indicated in panel D by arrows and the disulphide-forming cysteines are shown in panel F. Note that monomers I and III as well as II and IV, respectively, form the two hSSB1 dimers that recognise the oligo$(dT)_{12}$ ssDNA. The orientation of the structures in panels A, B, C and D is identical to Figure 3C and 5C.

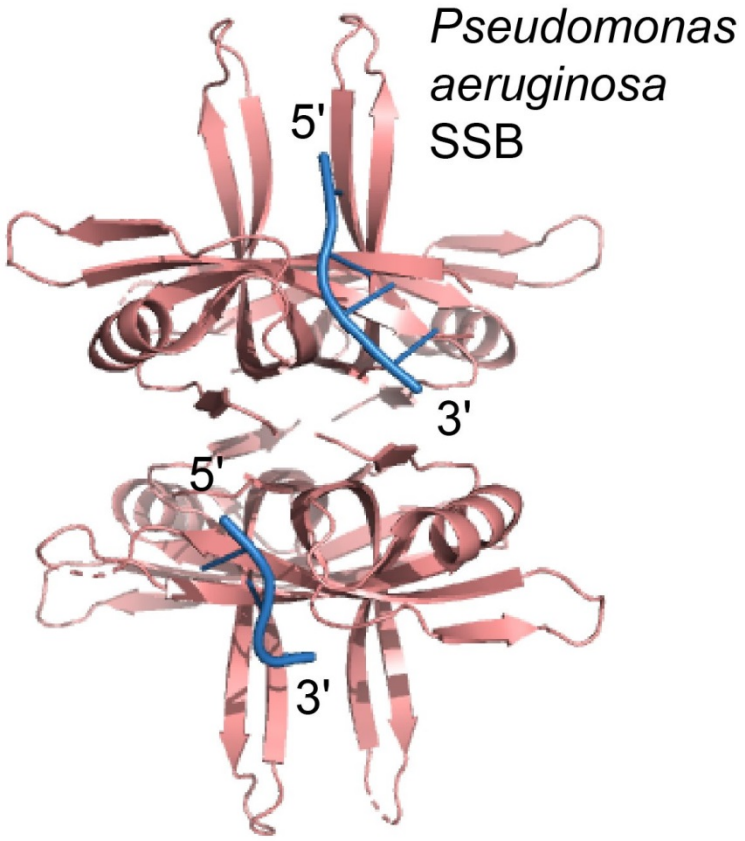

Figure 8. Structure of *Pseudomonas aeruginosa* SSB bound to ssDNA. X-ray crystal structure of tetrameric *P. aeruginosa* SSB (salmon) bound to ssDNA (blue) at 1.91 Å resolution (PDB ID 6IRQ) (43). Note that both ssDNA binding polarities exist in the structure (only the relevant ssDNA from PDB ID 6IRQ is shown).

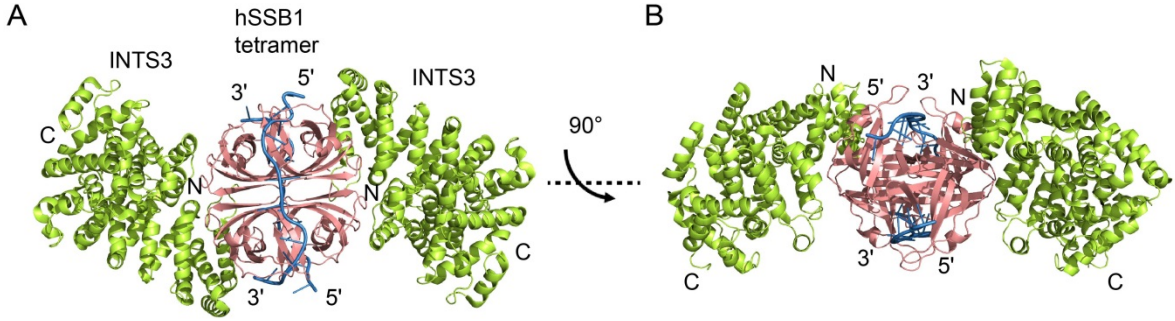

Figure 9. Structural model of hSSB1-ssDNA-INTS3 complex. Structural model of a complex between tetrameric hSSB1 (salmon), ssDNA (blue) (hSSB1 model (3); Figure 7D-E) and the N-terminus of INTS3 (green). Note that one out of four possible conformers is shown.